Optik 127 (2016) 4726–4730

Contents lists available at ScienceDirect

Optik

journal homepage: www.elsevier.de/ijleo

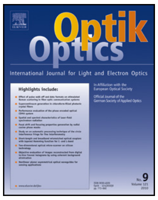

Effect of copper precursor salts: Facile and sustainable synthesis of controlled shaped copper oxide nanoparticles

Hafsa Siddiqui, M.S. Qureshi, Fozia Z. Haque*

Optical Nanomaterials Lab, Department of Physics, Maulana Azad National Institute of Technology, Bhopal 462051, India

ARTICLE INFO

Article history:
Received 30 November 2015
Accepted 14 January 2016

Keywords:
Sustainable protocol
Copper oxide
Copper salts
Chemophysical properties

ABSTRACT

A facile and sustainable protocol for the synthesis of copper oxide (CuO) nanoparticles has been developed successfully. This synthesis protocol has been comparatively easy to implement and could contribute to overcome the challenge of obtaining numerous morphologies of CuO in efficient and sustainable routine. Different shapes of CuO nanoparticles have been synthesized via simply changing the precursor copper salts such as copper nitrate ($Cu(NO_3)_2$), and copper chloride ($CuCl_2$) with the same synthetic protocol. Herein, a comparative study has done in between structural, morphological and optical properties of as synthesized CuO nanoparticles. XRD analysis indicated that nanoparticles closely resembled and had monoclinic CuO nanocrystals. The FESEM result demonstrates that morphology of particles obtained is mainly due to the precursor salts. Both prepared CuO particle using either $Cu(NO_3)_2$ or $CuCl_2$ are in good dispersion and found to be in nanometer size. The $CuCl_2$ gives the highly dense packed mixed morphology of cubic and sphere shaped particles. Whereas ($Cu(NO_3)_2$ shown only flakes like morphology. FTIR analysis proposed the reacting process which described the corresponding vectorial relations between crystal parameters. Copper hydroxide gives rise to oxide through the formation of a $Cu(NH_3)^{2+}{}_4$, by a reconstructive transformation involving a dissolution reaction followed by a precipitation. The optical properties of both samples show several emission peaks in visible spectrum range. All characterization results revealed that chemophysical properties of CuO nanoparticles are highly dependent on Cu salts.

1. Introduction

Not only the size, but shape of nanomaterials exerts tremendous impact on their properties. Shape changes the exposed crystal facets and hence the atomic arrangements in each facets which will have intense effect on its various properties [1–3]. CuO nanomaterials have been showing broadened applications in the field sensing, electronics, magnetic storage media, semiconductor and solar cells owing to its photoconductive and photochemical properties [4–14]. Recently, copper (II) oxide has been explored to be a new class of electrode material for rechargeable lithium-ion batteriesand photocatalysts [9–11]. The synthesis method of CuO nanostructures varies from case to case. The solution-phase synthesis approaches are considered as one of the promising routes for the fabrication of CuO nanostructures with different morphologies such as nanowire, nanoribbons, nanosheets, nanotubes, nanorods, etc. [1–3], due to its low cost, high yield and high quality production [12]. Among the synthesis protocols, the surfactant assisted method has advantages it offer controlled shape morphology as well as the dispersion in various media. Several CuO nanostructures have been synthesized by this way [15–17]. However, most of these synthesis protocols can only produce one or two morphologies. A systematic study on one-pot way synthesis of various morphologies CuO nanostructures is limited, and it's still a big challenge to develop facile and sustainable synthetic protocol for the controlled synthesis of different shaped CuO nanostructures. In principle, any kind of soluble copper salts could be used as precursor to prepare CuO nanostructures without modification or at least there seems to be very few reports on the influence of copper salt precursor. Various copper salts such as chloride, nitrate, sulfate and acetate were used to prepare CuO nanomaterials; however the effect of different copper salts were not discussed in details. In continuation of our work on synthesis and morphology controlled oxide nano-material [15–21] here, we report facile and sustainable synthesis of CuO nanostructures that were produced by using exactly same synthetic protocol with simply changing the copper salt. A comparative study between two different copper salts such as copper nitrate ($Cu(NO_3)_2$), copper and copper

---

* Corresponding author. Tel.: +91 9300687943.
E-mail address: foziazia@rediffmail.com (F.Z. Haque).

http://dx.doi.org/10.1016/j.ijleo.2016.01.118

chloride ($CuCl_2$) were done to check the effects of precursors on CuO. The crystallographic parameters, structure, chemical and optical properties of the as-synthesized CuO samples were seen a significant changes in the chemophysical and optical properties.

2. Experiment detail

2.1. Synthesis methods

All the chemicals used in the experiment were analytical reagent grade and were used without further purification. The different shapes of CuO nanoparticles was synthesized via water based simple synthesis protocol, which involves copper (II) nitrate trihydrate ($Cu(NO_3)_2{\cdot}3H_2O$, Merck, ≥98%) and copper(II)chloride dihydrate ($CuCl_2{\cdot}2H_2O$, ACS reagent, ≥99.0%) as copper-precursors, hexamethylenetetramine (HMT, $C_6H_{12}N_4$, ACS reagent, ≥99.0%) as surfactant, water as reaction solvent and sodium hydroxide (99.5%, NaOH, Merck, ≥98%) as hydrolyzing agent.

2.1.1. Sample 1

Stoichiometric ratio of $Cu(NO_3)_2{\cdot}3H_2O$ (0.1 mol) was dissolved in 400 ml deionized water and allowed to stirrer at 50 °C, followed by the drop-wise addition of HMT into the reaction mixture, that an aqueous solution of sodium hydroxide was gradually added until the precursor reached pH value at 9. Resultant solution was subjected to magnetic stirring at 50 °C until uniform brown-black solution was formed, followed by the heating for 5 h in hot air oven at 110 °C. After cool down at room temperature the obtained precipitate was washed several times with ethanol and dried at room temperature.

2.1.2. Sample 2

The synthesis condition and reaction time was same as above, only change the Cu salt using (0.1 mol) $CuCl_2{\cdot}2H_2O$ instant of $Cu(NO_3)_2{\cdot}3H_2O$. Finally, crystalline CuO powdered samples were obtained after calcined process in hot air oven at 200 °C for 5 h.

2.2. Characterization details

The crystal structure, phase and crystallite sizes of obtained samples were characterized by powder X-ray diffraction (XRD) analysis on D8-Advance (Bruker, Germany) X-ray diffractometer system with Cu-$K_{\alpha 1}$ radiation (λ = 1.5406 Å). Their morphology and microstructures were characterized by field emission scanning electron microscopy (FESEM, TESCAN) and transmission electron microscopy (TEM) at room temperature, using modal TECNAI-G^2, apparatus working at 200 kV. The chemical information including various vibrational modes which are present in the prepared samples was examined via energy-dispersive X-ray (EDX) analyzer which was attached with JEOL-JSM-6390 scanning electron microscopy and fourier transform infrared spectroscopy (Bruker Vertex 70 FTIR) spectrophotometer in the range of 4000–400 cm^{-1} at the resolution of 0.5 cm^{-1}. Optical properties of the samples were determined by using PL spectroscopic (F-7000 Hitachi).

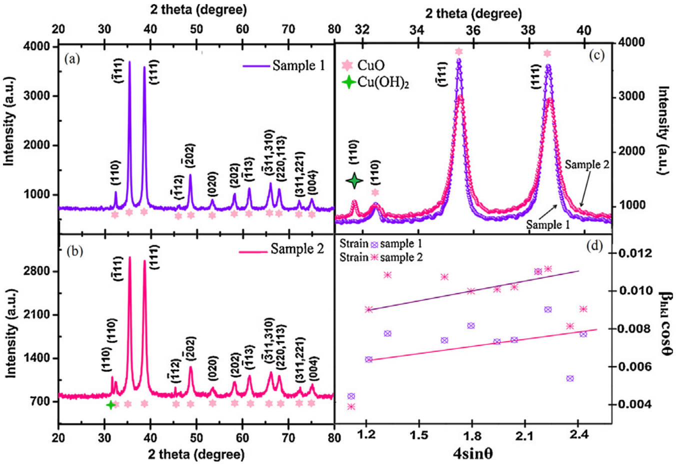

Fig. 1. The X-ray diffraction patterns of as-prepared: (a) sample 1; (b) sample 2; (c) the XRD pattern of the three most intense plans of both samples; (d) W–H plot of both as prepared samples assuming UDM with fit to the data strain extracted from the slope.

3. Results and discussion

3.1. Crystal structure and phase analysis

The XRD patterns of both as-synthesized samples have been recorded in the diffraction angle range 20–80° and are shown in Fig. 1. The XRD profile strongly shows crystalline natures of sample 1 (CuO nanoflakes) compared to the sample 2 (CuO nanoparticles). It was confirmed that the structure of sample 1 have single phase CuO monoclinic crystal structure with space group *C2/c* (Fig. 1(a)). Whereas in case of sample 2 the characteristic peaks located at 2 theta 31.54° was assigned to (110) plan of $Cu(OH)_2$ which belongs to an orthorhombic type crystal structure and had a space group *Cmcm* (JCPDS #80-13-0424, see in Fig. 1(b)). The XRD peaks were well-indexed with standard JCPDS #80-1916. The interplanar spacing ‘*d*’ and lattice parameters ($a \neq b \neq c, \alpha = \gamma = 90^\circ \neq \beta$ for monoclinic structure) were evaluated from Eqs. (1) and (2). The obtained data were summarized in Table 1.

$$n\lambda = 2d \quad \sin \quad \theta \tag{1}$$

$$\frac{1}{d^2} = \frac{1}{\mathrm{Sin}^2 \quad \beta}\left(\frac{h^2}{a^2} + \frac{\sin^2 \quad \beta}{b^2} + \frac{1^2}{c^2} - 2hl \quad \cos \quad \frac{\beta}{ac}\right) \tag{2}$$

It was reported that the ($\bar{1}11$) plane is more intense than the (111) plane, the growth of the particles are more favorable in the ($\bar{1}\bar{1}11$) direction than (111) direction [2]. XRD data show that the interplanar spacing (*d*-spacing) of ($\bar{1}11$) and (111) planes of sample 1 was higher comparing to sample 2 (Fig. 1(c)), due to the change in bond length and bond angle between Cu and O atoms that generate the lattice strain in materials. It was simply defined as the ratio of the incremental change of the lattice parameter to its initial value. Consequently, the lattice strain changes the spacing of crystallographic planes (*d*-spacing). According to Bragg’s Law, the Bragg angles should either decrease or increase when spacing of the

Table 1
Obtained Lattice parameters, crystallite size, microstrain and dislocation density of both samples were calculated by the following ref. [15] and compared with standard CuO JCPDS file no. 80-1916.

Code	2θ (°)			‘*d*’ spacing (Å)			Crystallite size ‘*D*’ (nm)	Microstrain ($\times 10^{-3}$)	Dislocation density ‘δ’ ($\times 10^{15}$ lines/m^2)
	(110)	($\bar{1}11$)	(111)	(110)	($\bar{1}11$)	(111)			
JCPDS	32.47	35.49	38.68	2.754	2.527	2.325			
Sample 1	32.46	35.49	38.72	2.763	2.536	2.331	19	0.419	0.0030
Sample 2	32.47	35.46	38.70	2.763	2.534	2.330	16	0.533	0.0048